NKS-387
ISBN 978-87-7893-473-4

Development of a hybrid neutron transport solver in 2 energy groups

Sebastian Carbol[1]
Mikael Andersson[1]
Christophe Demazière[1]
Jaakko Leppänen[2]

[1]Chalmers University of Technology, Sweden

[2]Technical Research Centre of Finland (VTT)

April 2017

Abstract

This project investigates the feasibility of performing reactor physics calculations for nuclear cores using a hybrid neutron transport methodology, by combining deterministic and probabilistic modelling techniques. In the presented implementation, a deterministic response matrix method was developed in Matlab. The necessary probabilities appearing in the response matrix method were estimated in advance using a probabilistic solver – the Monte Carlo code Serpent2. Ultimately, the hybrid framework will combine the advantages of the deterministic approach (fast running calculations) with the ones of the probabilistic approach (high flexibility in modelling any geometry and high accuracy). In the response matrix method, two grids are used: one fine grid for estimating the scalar neutron flux and a coarse grid for computing the neutron currents on this grid. Because of the large efforts developing a new computational framework represents and because such a developmental work is error-prone, this first phase of the project implemented and tested the hybrid framework on a system as simple as possible: a two-dimensional representation of a simplified BWR fuel assembly. Such a choice was governed by the necessity to lower the computational time and to have a tractable system during the developmental phase of the framework. The development of the hybrid route was demonstrated to be feasible, after some modifications of the Serpent2 code. Although promising, the solution computed by the framework was demonstrated to be not fully realistic. Additional investigations are necessary to identify the root cause of the observed deviations from the expected physical behaviour of the system.

Key words

nuclear reactor calculations, neutron transport, deterministic methods, probabilistic methods, hybrid methods

NKS-387
ISBN 978-87-7893-473-4
Electronic report, April 2017
NKS Secretariat
P.O. Box 49
DK - 4000 Roskilde, Denmark
Phone +45 4677 4041
www.nks.org
e-mail nks@nks.org

Development of a hybrid neutron transport solver in 2 energy groups

Final Report from the NKS-R HYBRID activity

(Contract: AFT/NKS-R(16)120/7)

Sebastian Carbol[1]
Mikael Andersson[1]
Christophe Demazière[1]
Jaakko Leppänen[2]

[1]Chalmers University of Technology, Department of Physics, Division of Subatomic and Plasma Physics, SE-412 96 Gothenburg, Sweden
[2]Technical Research Centre of Finland (VTT), P.O. Box 1000, FI-02044 VTT, Finland

Table of contents

	Page
1. Introduction	1
2. Survey of the field	2
3. Theoretical framework	4
4. Description of the test system	7
5. Implementation	8
5.1 Estimation of the required probabilities	8
5.1.1 Neutrons entering through a surface	9
5.1.2 Neutrons emitted from a region	11
5.2 Labelling of the system	12
5.3 Structure of the computational framework	14
5.3.1 Building of the matrix $\mathbf{R}$	15
5.3.2 Building of the matrix $\mathbf{P}$	16
5.3.3 Building of the matrix $\mathbf{S}$	16
5.3.4 Building of the matrix $\mathbf{F}$	17
5.3.5 Estimation of the emission density Q	18
5.3.6 Estimation of the source terms ϕ_{source} and $\mathbf{J}_{source}$	19
6. Results	19
6.1 Results from the probabilistic framework	19
6.2 Results from the deterministic framework	22
7. Conclusions and outlook	24
8. References	25

Acknowledgements

NKS conveys its gratitude to all organizations and persons who by means of financial support or contributions in kind have made the work presented in this report possible.

Disclaimer

1. Introduction

The modelling of neutron transport problems for radiation transport purposes and nuclear reactor systems has long been divided into two types of approaches: the deterministic approach and the probabilistic approach.

In the deterministic approach, the neutron transport equation is solved explicitly after reducing the complexity of the task at hand (typically using space-homogenization, energy-condensation, and angular discretization techniques) (Demazière, 2013). The problem is first solved in a very small part of the computational domain using proper boundary conditions, and the solution then computed is used for transforming the problem into a problem encompassing a larger computational domain, at the expense of a simplification of the true complexity of the system. Typically, three to four of such "bottom-up" simplifications are used to model a full reactor core. Nevertheless, the validity of the approximations used in each of the computational steps are never corrected by the results of the calculations performed at the following computational step when a better (i.e. taking a larger computational domain into account) solution has been computed. Such methods are fast-running methods originally developed when the computing resources were limited.

In the probabilistic approach, also referred to as Monte Carlo, no equation as such is solved. Rather, the probability of occurrence of a nuclear reaction/process of a given type on a given species at a given energy for a given incoming particle (which can still exist after the nuclear interaction) is used to sample neutron life histories throughout the system (Lux and Koblinger, 1991). Using a very large number of such histories, the true behaviour of neutrons in the system can be reproduced. Due to the size and complexity of the systems usually modelled, Monte Carlo techniques are extremely expensive computing techniques, originally used for reference and shielding calculations.

With the development of cheap computing resources, both the deterministic approach and the probabilistic approach are currently being used on massively parallel clusters to circumvent the limitations mentioned above. In the deterministic case, the process of averaging ("bottom-up") is now being complemented by a de-averaging process ("top-down") in an interactive manner, so that a better modelling of the boundary conditions can be achieved using the information available from the coarser mesh. The modelling of full cores in one computational step only is also being attempted. In the probabilistic case, the use of large clusters allows modelling full reactor cores, and efforts are being pursued to include the effects induced by changes in the composition and/or density of the materials. Due to the complexity and level of details in the deterministic approach based on the averaging/de-averaging process, the deterministic route has become as computationally expensive as the probabilistic route for high-fidelity simulations.

The present project proposes to combine deterministic methods with probabilistic methods. The main advantage of such a *hybrid* route would be to lower the computational cost of the calculations (thanks to the use of deterministic methods) while still guaranteeing a high level of details and of reliability of the calculations (thanks to the use of probabilistic methods). A promising candidate for such a hybrid route is to use the so-called response matrix method, also known as the interface current method (Stacey, 2001; Stamm'ler RJJ & Abbate MJ). This method is essentially a deterministic method, where two computational grids are used: one coarse grid for resolving the neutron currents between the thus-defined cells (assuming that the neutron emission densities are known within the cells), and one finer grid for resolving

within each cell the neutron emission densities (assuming that the neutron currents between cells are known). The solutions of the two grids are iteratively updated until convergence is reached. The application of such a method requires the prior determination of some specific probabilities within each cell. The prior determination of the necessary probabilities is a very difficult task, because of the three-dimensional nature of the problem at hand and of the possible geometrical complexity of the system.

The present project thus proposes:

- To determine using a Monte Carlo code the required collision probabilities for the response matrix method.
- To develop a software for testing the response matrix method using Monte Carlo-generated collision probabilities.

Because of the large efforts developing a new computational framework represents and because such a developmental work is error-prone, it was decided in the first phase of the project to keep the system as simple as possible. With the objectives to lower the computational time and to have a tractable system, only two-dimensional systems representative of fuel assemblies having a regular lattice of fuel pins surrounded by coolant were thus considered. This also means that the fine grid was chosen as made of a fuel pin and its associated coolant and the coarse gird was correspondingly made of the juxtaposition of such cells.

In a later phase of the project, the method will be tested on three-dimensional systems representative of an entire nuclear core (with the coarse grid being of the size of axial slices of fuel assemblies and the fine grid modelling the spatial inhomogeneity within such slices of fuel assemblies).

2. Survey of the field

The governing equation for neutron transport is given by the neutron transport equation or Boltzmann equation. Due to the integro-differential/integral nature of the equation, the number of variables to be resolved and the usual large size of the system, the Boltzmann equation is ultimately simplified into a simpler formalism based on multi-group diffusion theory when a deterministic framework is used. The balance equations are then integrated on small volumes (finite volume approach) and on small energy bins (multi-group approach), and dedicated solution procedures are used for resolving the spatial, temporal, and energy distribution of the neutrons (Demazière, 2013). One of the major obstacles in this modelling procedure is that the balance equations make use of spatially- and energy-integrated macroscopic nuclear cross-sections. In order to properly homogenize (i.e. average in space) and condense (i.e. average in energy) such cross-sections, the nuclear reaction rates have to be preserved during such a double averaging procedure, and the scalar neutron flux used as a weighting function. Since the scalar neutron flux is the quantity one wants to determine and because of the parabolic nature of the neutron diffusion equations, which requires to solve the entire problem, a multi-step computational approach is used in deterministic neutron transport. A very small part of the computational domain is first considered, and assumptions on the surrounding of this domain and on the entry of the neutrons at the boundary of this domain are made. The neutron transport equation is then used to determine a good enough guess of the neutron flux, so that the macroscopic cross-sections can be properly homogenized and condensed. The main approximations and limitations used in the multi-level

computing scheme highlighted above are manifold. The most important one lies with the fact that the calculations performed on a restricted part of the domain rely on many intertwined steps where some approximations about the re-entry of neutrons at the boundaries of the domain are necessary. Such approximations are considered to be the main limitation in reaching highly accurate results for deterministic neutron transport (Roberts et al., 2010).

To circumvent the limitations highlighted above, large international efforts in the area of both deterministic neutron transport and probabilistic neutron transport are on-going. On the deterministic side, one can refer to the Consortium for Advanced Simulation of Light Water Reactors (CASL) Energy Innovation Hub sponsored by the Department of Energy in the USA (U.S. Department of Energy, 2015b) and to the Center for Exascale Simulation of Advanced Reactors (CESAR) (U.S. Department of Energy, 2015a). Such initiatives intend to make use of world-class computing techniques thus allowing to use fine-mesh (in space, energy, and angle) neutron transport methods without using a classical multi-step procedure as highlighted above (see e.g. Davidson et al., 2014 and Boyd et al., 2013 for CASL and CESAR, respectively). On the probabilistic side, one can mention the EU-sponsored project High performance Monte Carlo reactor core analysis (HPMC), where high performance computing techniques are used to resolve the interdependence between neutron transport, material properties and compositions (Ivanov, 2014; Dufek & Anglart, 2014; Dufek & Hoogenboom, 2014).

Other international efforts in the area of hybrid methods are also on-going, although on a much more limited scale compared to full use of deterministic methods or full use of probabilistic methods and the corresponding projects in these areas. The one driven by Georgia Institute of Technology, USA (Zhang & Rahnema, 2012), with the development of the COMET code (Coarse Mesh Transport), makes use of the computation of "response functions", i.e. the response of a given cell to an incoming angular neutron flux. Such responses are computed using a Monte Carlo code assuming different expansions with respect to angle, space, and energy of the angular neutron flux. In addition, the effective multiplication factor of the system is an input to the Monte Carlo simulations. Similar efforts were initiated by Hitachi some years ago (Moriwaki et al., 1999; Ishii et al., 2009). Other efforts, such as the ones led by and in collaboration with MIT, USA (Lee et al., 2014; Li et al., 2014) and the University of Michigan, USA (Wolters et al., 2011), in the area of hybrid methods, focus on the acceleration of the convergence of the fission source in full core Monte Carlo simulations using a full core low-order deterministic approach.

In the present project, it is proposed to use the response matrix method in a deterministic sense while using a Monte Carlo solver to estimate the required probabilities. Even if the proposed method belongs to the same class of methods as the effort led by Georgia Tech, the implementation proposed here is radically different. Namely, the Monte Carlo code is used to directly compute within-cells probabilities, and the response matrix method would be applied both at the fine mesh and the coarse mesh levels to resolve neutron fluxes and neutron currents once such probabilities are determined. The main advantage of this implementation is the fact that the effective multiplication does not need to be used as an input parameter in the Monte Carlo runs, as is the case of the method developed by Georgia Tech. In addition, the proposed implementation opens the possibility of performing the computation of the probabilities in three dimensions directly, due to the small size of the computational domain considered for the within cells-Monte Carlo simulations.

3. Theoretical framework

In order to better highlight the proposed method, the neutron transport equation is recalled hereafter, and the balance equations in the response matrix formalism are derived. Using standard notations in multi-energy group theory and using a classical transport correction of the total and scattering macroscopic cross-sections, the steady-state transport equation in its integral form written for the energy group g reads as (Stamm'ler and Abbate, 1983):

$$\psi_g\left(\mathbf{r},\overline{\Omega}\right) = \int_0^{\infty} \exp\left[-\int_0^s \Sigma_{T,g}^0\left(\mathbf{r}-s'\overline{\Omega},E\right)ds'\right] \times q_g\left(\mathbf{r}-s\overline{\Omega},\overline{\Omega}\right)ds \tag{1}$$

where the emission density is given by:

$$q_g\left(\mathbf{r},\overline{\Omega}\right) = \frac{1}{4\pi}\sum_{g'=1}^{G}\left[\Sigma_{s0,g'\to g}^0\left(\mathbf{r}\right) + \chi_g \frac{\upsilon\Sigma_{f,g'}\left(\mathbf{r}\right)}{k_{eff}}\right]\phi_{g'}\left(\mathbf{r}\right) \tag{2}$$

Partitioning the volume V of the system into sub-volumes V_i, such that $V = \bigcup_i V_i$, and partitioning the outer surface S of the system into sub-surfaces S_a, such that $S = \bigcup_a S_a$, multiplying Eq. (1) by the transport-corrected total cross-section, assuming a homogeneous emission density on each sub-volume and integrating on one of the sub-volumes V_i lead to:

$$\Sigma_{T,g,j}^0 \phi_{g,j} V_j = \sum_a S_a J_{in,g,a} P_{g,a\to j} + \sum_i V_i Q_{g,i} P_{g,i\to j} \tag{3}$$

where the emission density in energy group g and region i is given by:

$$Q_{g,i} = \frac{1}{4\pi}\sum_{g'\to 1}^{G}\left[\Sigma_{s0,g'\to g,i} + \frac{\chi_{g',i}\nu\Sigma_{f,g',i}}{k_{eff}}\right]\phi_{g',i} \tag{4}$$

Taking again Eq. (1) this time at the outer boundary of the system, multiplying this equation by $\left|\overline{\Omega}\cdot\overline{n}\right|$, assuming a homogeneous emission density on each sub-volume and integrating on a given surface S and for solid angles such that $\overline{\Omega}\cdot\overline{n} > 0$ lead to:

$$S_a J_{out,g,a} = \sum_b S_b J_{in,g,b} P_{g,b\to a} + \sum_i V_i Q_{i,g} P_{g,i\to a} \tag{5}$$

In the previous two equations, the different quantities have the following meaning:

- $J_{in,g,a}$ and $J_{out,g,a}$ represent the averaged incoming, outgoing respectively, neutron currents on the surface area S_a.
- $P_{g,i\to j}$ represents the probability for a neutron emitted in the volume V_i in an isotropic manner and having a given emission density to have its first collision in the volume V_j.
- $P_{g,a\to j}$ represents the probability for a neutron entering through the surface S_a to have its first collision in the volume V_j.

- $P_{g,i\to a}$ represents the probability for a neutron emitted in the volume V_i in an isotropic manner and having a given emission density to escape without interaction through the surface S_a .
- $P_{g,b\to a}$ represents the probability for a neutron entering through the surface S_b to escape without interaction through the surface S_a .

The above system of equations has nevertheless very limited practical usefulness since for a large system, the number of probabilities to be computed would be enormous. The essence of the response matrix method is thus to use two computational grids. If one considers that the system to be studied contains $I = 1,...,N$ sub-systems, each having respectively a volume V_I delimited by a surface S_I, Eqs. (3) and (5) can be written on each of the sub-systems as:

$$\Sigma^0_{T,g,j}\phi_{g,j}V_j = \sum_{a\in S_I} S_a J_{in,g,a,} P_{g,a\to j} + \sum_{i\in V_I} V_i Q_{g,i} P_{g,i\to j} \quad \text{for } j \in V_I \tag{6}$$

$$S_a J_{out,g,a} = \sum_{b\in S_I} S_b J_{in,g,b} P_{g,b\to a} + \sum_{i\in V_I} V_i Q_{g,i} P_{g,i\to a} \quad \text{for } a \in S_I \tag{7}$$

If $\mathbf{J}^I_{out}$ represents the vector having for components each of the currents $J_{out,a}$ on all sub-surfaces belonging the boundary of the sub-system I, if $\mathbf{J}^I_{in}$ represents the vector having for components each of the currents $J_{in,a}$ on all sub-surfaces belonging the boundary of the sub-system I, and if $\mathbf{J}^I_{source}$ represents the vector having for components the contribution to the current $J_{out,a}$ due to volumetric sources inside the sub-system I, the set of equations (6) can be recast in the following vector equation:

$$\mathbf{J}^I_{out} = \mathbf{R}^I \times \mathbf{J}^I_{in} + \mathbf{J}^I_{source} \tag{8}$$

where $\mathbf{R}^I$ is referred to as the response matrix for the sub-system I. Such a vector equation can be written for any sub-system I of the computational domain, and thus one can write:

$$\mathbf{J}_{out} = \mathbf{R} \times \mathbf{J}_{in} + \mathbf{J}_{source} \tag{9}$$

for the entire system being modelled. In this equation, $\mathbf{R}$ is referred to as the response matrix for the entire system. Since the outgoing current from a given sub-system is equal to the incoming current to its neighbouring sub-system, a topographical relationship exists between $\mathbf{J}_{in}$ and $\mathbf{J}_{out}$ which can be generically written as:

$$\mathbf{J}_{in} = \mathbf{P} \times \mathbf{J}_{out} \tag{10}$$

where $\mathbf{P}$ is a matrix defined for the entire system being considered. Combining Eqs. (9) and (10) leads to:

$$\mathbf{J}_{in} = \mathbf{P} \times \mathbf{R} \times \mathbf{J}_{in} + \mathbf{P} \times \mathbf{J}_{source} \tag{11}$$

This equation represents the *global* problem, i.e. the problem defined for the entire computational domain. Likewise, Eq. (6) can also be recast into the following vector equation:

$$\phi^I = \mathbf{S}^I \times \mathbf{J}^I_{in} + \phi^I_{source} \tag{12}$$

This equation represents the *local* problem, i.e. the problem defined for the sub-system I. The probabilities $P_{g,a\to j}$, $P_{g,i\to j}$, $P_{g,b\to a}$, and $P_{g,i\to a}$ need to be calculated prior to the application of the response matrix method. Nevertheless, compared to the original formulation of the transport problem as given by Eqs. (3) and (5), only probabilities within each sub-system need to be evaluated when two computational grids (i.e. a global problem and a local problem) are used. Once the different probabilities have been evaluated, the solution procedure goes as follows. From a known distribution of the emission densities for the entire computational domain, the global problem is solved, i.e. the neutron currents between each sub-system are computed using Eq. (11). Once the currents have been determined, the local problem is solved for each of the sub-systems, i.e. the scalar neutron fluxes within each sub-system are determined using Eq. (12). The calculated neutron fluxes within each sub-system are then used to calculate an updated distribution of the emission densities for the next inner iteration.

In this project, the Monte Carlo tool Serpent2 was used to evaluate the probabilities within each of the sub-systems for both the global and the local problems (Leppänen et al., 2015). Compared to the work carried out by Georgia Tech and Hitachi earlier mentioned where only the global problem was solved deterministically, the main difference lies with the fact that the local problem is also solved in a deterministic sense, while using probabilities estimated from a probabilistic route. The main advantage is that the effective multiplication factor of the system is not any longer a necessary a priori input to the Monte Carlo simulations, but can be calculated on-the-fly by the deterministic solution procedure, using a classical power iteration method (Stamm'ler and Abbate, 1983):

$$k^{(p)} = k^{(p-1)} \frac{\overline{x}^{(p-1)} \cdot \overline{x}^{(p)}}{\overline{x}^{(p-1)} \cdot \overline{x}^{(p-1)}} \tag{13}$$

where p represents the iteration number, k is the dominant eigenvalue of the system, and the vector $\overline{x}$ represents the result of the application of the fission operator onto the scalar neutron flux, i.e. $\overline{x} = \overline{\overline{F}}_{\phi} \times \overline{\phi}$. The components of this vector are formally given by:

$$x_{g,j} = \sum_{i\in V_i} V_i Q^{fission}_{g,i} P_{g,i\to j} = \sum_{i\in V_i} V_i P_{g,i\to j} \chi_{g,i} \sum_{g'} (\nu\Sigma_f)_{g',i} \phi_{g',i} \tag{14}$$

In addition, the computational burden of estimating the probabilities are left to the Monte Carlo tool. Because of the small sizes of the sub-systems, estimating such probabilities is relatively fast. Furthermore, the estimation of the probabilities represents independent tasks, and parallel computing techniques could be used to distribute the required calculations when large scale systems would have to be considered.

It has to be mentioned that such a hybrid solution procedure nevertheless relies on some necessary approximations for both the spatial and angular distributions of the angular neutron

flux at the boundaries between the different sub-systems (isotropic and homogeneous emissions).

4. Description of the test system

In order to guarantee a simple enough system in this developmental phase of the project, the method was applied on a system representative of an axial slice of a BWR fuel assembly (two-dimensional system). The fine grid (local problem) was chosen as made of a fuel pin and its associated coolant and the coarse gird (global problem) was correspondingly made of the juxtaposition of such cells.

In a later phase of the project, the method will be tested on three-dimensional systems representative of an entire nuclear core (with the coarse grid being of the size of axial slices of fuel assemblies and the fine grid modelling the spatial inhomogeneity within such slices of fuel assemblies).

For the sake of simplicity, the water gaps, cladding and fuel box were disregarded, resulting in a regular lattice of fuel pins for the system considered, as illustrated in Fig. 1.

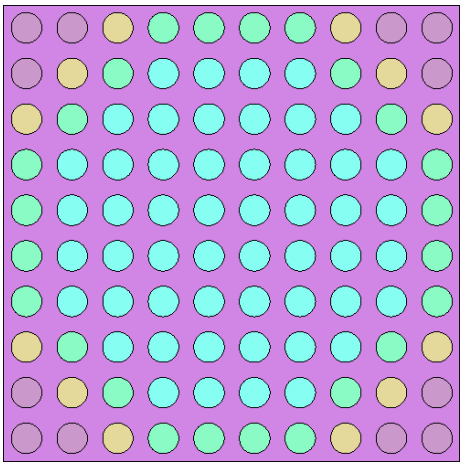

$$\begin{bmatrix} 2 & 2 & 3 & 5 & 5 & 5 & 5 & 3 & 2 & 2 \\ 2 & 3 & 5 & 6 & 6 & 6 & 6 & 5 & 3 & 2 \\ 3 & 5 & 6 & 6 & 6 & 6 & 6 & 6 & 5 & 3 \\ 5 & 6 & 6 & 6 & 6 & 6 & 6 & 6 & 6 & 5 \\ 5 & 6 & 6 & 6 & 6 & 6 & 6 & 6 & 6 & 5 \\ 5 & 6 & 6 & 6 & 6 & 6 & 6 & 6 & 6 & 5 \\ 5 & 6 & 6 & 6 & 6 & 6 & 6 & 6 & 6 & 5 \\ 3 & 5 & 6 & 6 & 6 & 6 & 6 & 6 & 5 & 3 \\ 2 & 3 & 5 & 6 & 6 & 6 & 6 & 5 & 3 & 2 \\ 2 & 2 & 3 & 5 & 5 & 5 & 5 & 3 & 2 & 2 \end{bmatrix}$$

Fuel pin number	U-235 [1]	U-238 [1]	O-16 [1]
1	0.015867	0.86563	0.1185
2	0.018512	0.86299	0.1185
3	0.022919	0.85858	0.1185
4	0.026445	0.85505	0.1185
5	0.029971	0.85153	0.1185
6	0.032615	0.84888	0.1185

Fig. 1 Radial layout of the modelled fuel assembly (left) with the corresponding fuel pin types (right) and their respective compositions (mass fractions of materials in the fuel pins).

The radius of each fuel pellet is 0.4335 cm and the fuel pin pitch is 1.295 cm. The fuel density is set to 10.424 g/cm^3. The moderator, assumed to be made of H_2O, has a density of 0.444 g/cm^3.

5. Implementation

In this section, the practical implementation of the chosen hybrid method is described. The method was applied to the case of 2 energy groups.

5.1 Estimation of the required probabilities

There are four probabilities that need to be determined for each subsystem, where a subsystem is made of a fuel pin and its surrounding coolant, as can be seen in Fig. 2. These are:

- $P_{g,i\to j}$: the probability for a neutron emitted in the volume V_i in an isotropic manner and having a given emission density to have its first collision in the volume V_j.
- $P_{g,a\to j}$: the probability for a neutron entering through the surface S_a to have its first collision in the volume V_j.
- $P_{g,i\to a}$: the probability for a neutron emitted in the volume V_i in an isotropic manner and having a given emission density to escape without interaction through the surface S_a .
- $P_{g,b\to a}$: the probability for a neutron entering through the surface S_b to escape without interaction through the surface S_a .

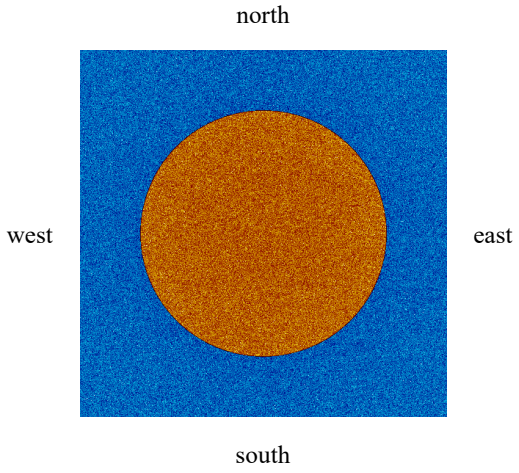

Fig. 2 Representation of an elementary subsystem (fuel region in red and coolant region in blue). Each subsystem has 4 surfaces defining its outer boundary (north, east, south, and west).

The estimation of these probabilities was carried out using Serpent2, using detectors, surfaces and materials, in combination with a newly introduced flagging feature. A surface detector is specified as:

det <detector name> ds <surface name> <direction>

The direction is defined differently depending on whether it is a plane surface or a surface of a geometry and is defined by a -1 or 1. For a plane, the direction is specified by the positive direction of the positive coordinate axis. For a geometry surface, the inward directions is defined as -1 and the outward direction as 1.

The flagging feature allows for setting and removing flags if a detector is scored and scoring a detector if a flag is or is not set. The flagging feature, called 'dfl' has two inputs and is written as follows:

$$\text{dfl} <\text{flag number}> <\text{option}>$$

where the 'flag number' is the number associated with a certain flag and the 'option' has four different inputs from 0 to 3:

- 0: remove the specified flag number when the detector is scored.
- 1: set the specified flag number when the detector is scored.
- -2/2: check if the specified flag number is set and score detector if set.
- -3/3: check if the specified flag number is set and score detector if not set.

Further, there is an option to set whether a series of 'dfl' tests act on an 'or' or an 'and' logic. This is done by setting a minus sign in front of the $<\text{option}>$.

It has to be mentioned that Serpent2 was also used to estimate the energy-averaged and region-averaged macroscopic data appearing in the deterministic computational framework.

5.1.1 Neutrons entering through a surface

The first set of probabilities to be determined are those due to neutrons entering the system through a surface. If looking at a specific surface a, any neutron entering through this surface must either leave the system again, through another surface, or react within the system, through scattering or absorption:

$$J_{in,a} = R_{moderator} + R_{fuel} + J_{out,2} + J_{out,3} + J_{out,4} \tag{15}$$

Normalising Eq. (15) with the current in through surface a the equation may be rewritten as:

$$\sum_{b \in S_I} P_{g,a \to b} + \sum_{i \in V_I} P_{g,a \to i} = 1 \tag{16}$$

This set of probabilities may be calculated by using a surface detector on one surface of the system, that measures the current of neutrons into the system, and setting flag 1 when this detector is scored.

$$\text{det surface\_A ds A 1 dfl 1 2}$$

This will calculate all neutrons entering the system through the west surface and will also be used as the normalisation to calculate the probabilities. The surface detectors can be seen in Fig. 3a. Two material detectors are used in the moderator and fuel, with the criteria that flag 1 is set, to count all neutrons that have entered through the west surface and that react in fuel

and moderator. These also have the ‘dfl’ setting that, when the detector is scored, flag 1 is removed, since after interacting with the system the neutron will be treated as coming from that region rather than from the west surface. These detectors are represented in Fig. 3c and Fig. 3b.

```
det fuel_interaction dm fuel1 dr -1 fuel1 dfl 1 2 dfl 1 0
det moderator_interaction dm cool dr -1 cool dfl 1 2 dfl 1 0
```

Four other surface detectors are used to calculate the current out of the system with the criteria that 1 flag is set. This will give the contribution from the west surface since any neutron that interacted with the system will lead to removal of flag 1 and hence will not be counted. The contributions are represented in Fig. 3d. The three surface detectors are defined as:

```
det surface_east ds east 1 dfl 1 2 dfl 1 0
det surface_south ds south -1 dfl 1 2 dfl 1 0
det surface_north ds north 1 dfl 1 2 dfl 1 0
```

Measuring the neutron current out through the west surface is not required, since only neutrons that did not interact with the system are counted and it is impossible for a neutron to enter and leave through the same surface without interacting within the system.

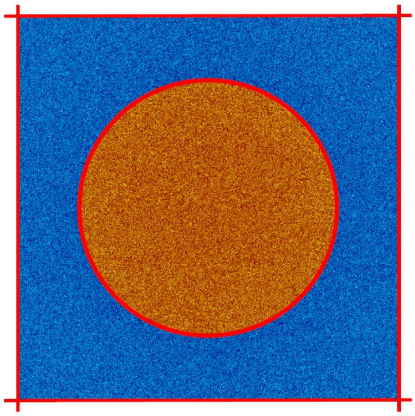

a) Outer surface detectors and surface detector around the fuel highlighted in red.

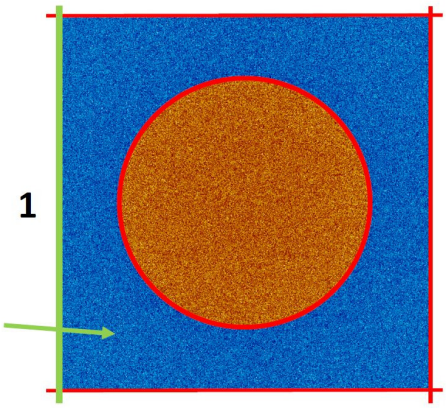

(b) Neutron entering through surface 1 and reacting in moderator.

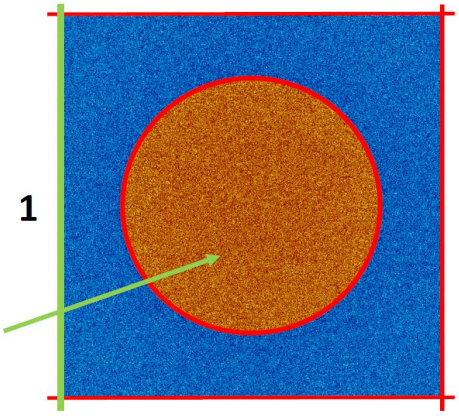

c) Neutron entering through surface 1 and reacting in fuel.

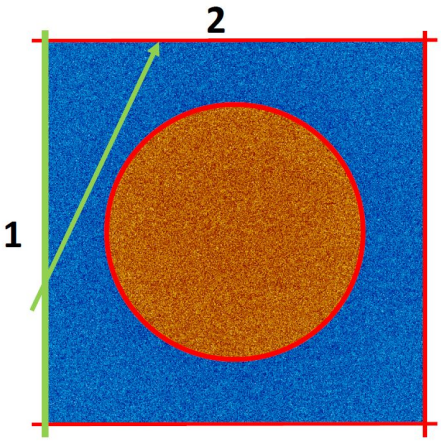

(d) Neutron entering through surface 1 and leaving through surface 2.

Fig. 3 Illustration of the different neutron paths for a neutron entering through a surface.

5.1.2 Neutrons emitted from a region

Similarly, two more sets of probabilities must be defined for neutrons being emitted from a region in the system. Since there are two regions, fuel and moderator, there will be two sets of probabilities that need to be calculated in Serpent2.

$$Emitted_{fuel} = R_{fuel} + R_{moderator} + J_{out,1} + J_{out,2} + J_{out,3} + J_{out,4} \tag{17}$$

and

$$Emitted_{moderator} = R_{moderator} + R_{fuel} + J_{out,1} + J_{out,2} + J_{out,3} + J_{out,4} \tag{18}$$

Both equations can be normalised by the total number of neutrons emitted, thus leading to:

$$\sum_{a\in S_I} P_{g,fuel\to a} + \sum_{i\in V_I} P_{g,fuel\to i} = 1 \tag{19}$$

and

$$\sum_{a\in S_I} P_{g,moderator\to a} + \sum_{i\in V_I} P_{g,moderator\to i} = 1 \tag{20}$$

The calculation of the probabilities above is more complicated than the previous sets of probabilities. The reason lies with the difficulty in tracking neutrons emitted in one region and having their first collision in the same region.

First, determining which neutrons were emitted from the region is difficult. The 'dfl' flagging feature does not allow for flagging source neutrons. This problem was remedied by adding a line of code to the source code in Serpent2: source neutrons were automatically flagged with flag number 1. Hence, calculating the number of neutrons emitted in a region and having their first interaction in the same region was simply calculated by checking all reactions in the material while flag 1 was set.

Then, the tracking of neutrons scattering in a region and thereafter first interacting in the same region is also a far from trivial task. This is treated as an emitted neutron in the response matrix method and hence needs to be determined. In Serpent2, however, no distinction is made between successive scattering events. To detect a following scattering event in a material, a flag would have to be set for the first scattering interaction. Nevertheless, after detecting a first scattering event, the second one would be scored as well since the scattering events happen within the same neutron history. This problem was solved by using the complementarity relationships given by Eqs. (19) or (20), i.e. using the fact all other the probabilities (i.e. other than the cumbersome probability) can be determined from Serpent2.

The calculation of all the contributions needed for the sets of Eqs. (19) and (20) is more complex and many detectors are needed with intricate 'dfl' flagging compositions. For the sake of clarity, such details are not presented here and the interested reader is referred to Carbol (2017).

5.2 Labelling of the system

Because of the local and global problems to be simultaneously solved in the response matrix method, a careful labelling of regions and surfaces is necessary. For illustration purposes, the labelling is demonstrated hereafter on a system made of 2x2 fuel pins.

The first step is to label all cells in the system. The labelling of a simple 2x2 system is given in Fig. 4.

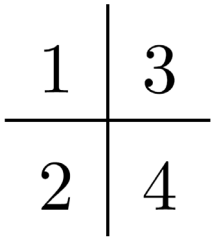

Fig. 4 Illustration of the labelling of cells.

The motivation to label the cells in this order is that the indexing of matrix elements in Matlab (which is the software used to implement the response matrix method in this work) is carried out in the same order and hence the cells can be accessed using one index only. The surfaces are numbered successively in order of each cell and going clockwise from the west surfaces in each cell. For the test system considered in this work, each cell has four surfaces belonging and in total there will be four times the number of cells surfaces, i.e. for a 2x2 system there will be 16 surfaces, as illustrated in Fig. 5.

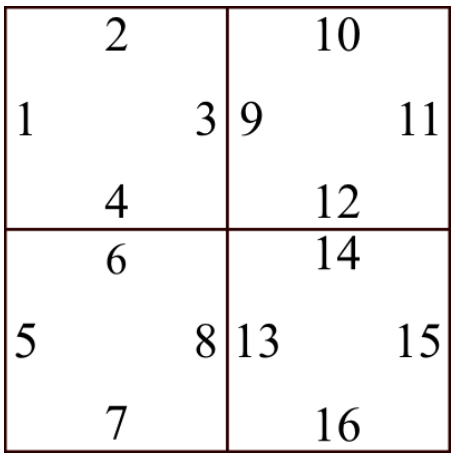

Fig. 5 Illustration of the labelling of surfaces.

Finally, in each cell, there are a given number of regions comprised of fuel or moderator, respectively. The regions are numbered successively following the numbering of each cell and going from the central region to the peripheral one. In the simplest case where there is only one fuel region and one moderator region and as illustrated in Fig. 6, the total number of regions is determined as the number of cells times the number of regions, i.e. for a 2x2 system there will be 8 regions.

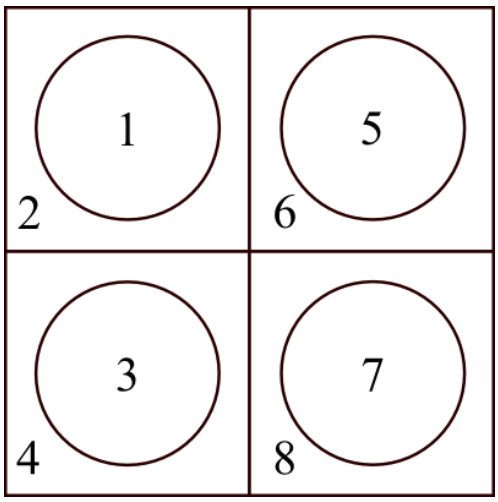

Fig. 6 Illustration of the labelling of regions.

5.3 Structure of the computational framework

The determination of the probabilities was carried out in advance using Serpent2. Such probabilities were thereafter used in a computational framework in Matlab using a response matrix formulation combined with a power iteration technique. The structure of the Matlab code is given in Fig. 7.

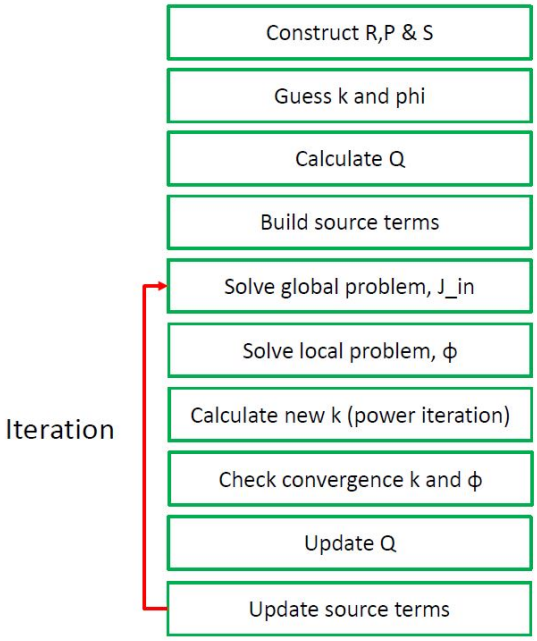

Fig. 7 Structure of the Matlab computational framework.

The building of the response matrix ($\mathbf{R}$), topological matrix ($\mathbf{P}$), local response matrix ($\mathbf{S}$) and fission matrix ($\mathbf{F}$) is first required to apply the proposed framework. The matrices only need to be determined once for the system used and can be computed in separate functions. The second step is to make an initial guess for the multiplication factor k and the scalar neutron flux. This allows calculating an initial neutron emission density Q. Using the neutron emission density, the source terms can be calculated as well as the source current and the source flux, which are used in the global and local problems, respectively.

The first step in the iteration is to solve the global problem to determine the currents into the system, $\mathbf{J}_{in}$ according to Eq. (11) which is recalled hereafter:

$$\mathbf{J}_{in} = \mathbf{P} \times \mathbf{R} \times \mathbf{J}_{in} + \mathbf{P} \times \mathbf{J}_{source} \tag{21}$$

Next, the local problem is solved for ϕ using $\mathbf{J}_{in}$ according to Eq. (12) also recalled hereafter and dropping the subsystem superscript I for the sake of clarity:

$$\phi = \mathbf{S} \times \mathbf{J}_{in} + \phi_{source} \tag{22}$$

Using the scalar neutron flux, a new multiplication factor k may be calculated using the power iteration method and the fission matrix $\mathbf{F}$. After a new k has been determined, the convergence can be checked with respect to both the scalar neutron flux and the effective multiplication factor. In both cases, the relative maximum difference between two iterations is

used to check convergence. If the iteration has not converged, the emission density is updated, leading to new source terms and the calculations will proceed in the same manner as earlier explained.

5.3.1 Building of the matrix $\mathbf{R}$

The response matrix $\mathbf{R}$ relates the outgoing neutron currents to the ingoing neutron currents. The response matrix is a square matrix of size $n \times n$, where n represents the total number of ingoing currents. Since the calculations are done with 2 energy groups there will be a response matrix related to each energy group. The structure of the response matrix can be determined from Eq. (7). The elements of the response matrix correspond to the ratios between the surface areas S_b and S_a times the probability to go from surface S_b to S_a.

Looking at one single subsystem I and the contribution to one surface, the terms contributing to the response matrix will be determined by:

$$S_a J^I_{out,g,a} = S_{b_1} J_{in,g,b_1} P_{g,b_1 \to a} + S_{b_2} J_{in,g,b_2} P_{g,b_2 \to a} + S_{b_3} J_{in,g,b_3} P_{g,b_3 \to a} + S_{b_4} J_{in,g,b_4} P_{g,b_4 \to a} \tag{23}$$

In the case where the surface areas are equal (as in the present application of the framework), the equation above becomes:

$$J^I_{out,g,a} = J_{in,g,b_1} P_{g,b_1 \to a} + J_{in,g,b_2} P_{g,b_2 \to a} + J_{in,g,b_3} P_{g,b_3 \to a} + J_{in,g,b_4} P_{g,b_4 \to a} \tag{24}$$

Casting this equation into a matrix equation shows the structure of the response matrix for a subsystem I:

$$\begin{bmatrix} J_{out,g,1} \\ J_{out,g,2} \\ J_{out,g,3} \\ J_{out,g,4} \end{bmatrix} = \begin{bmatrix} P_{g,a_1 \to a_1} & P_{g,a_2 \to a_1} & P_{g,a_3 \to a_1} & P_{g,a_4 \to a_1} \\ P_{g,a_1 \to a_2} & P_{g,a_2 \to a_2} & P_{g,a_3 \to a_2} & P_{g,a_4 \to a_2} \\ P_{g,a_1 \to a_3} & P_{g,a_2 \to a_3} & P_{g,a_3 \to a_3} & P_{g,a_4 \to a_3} \\ P_{g,a_1 \to a_4} & P_{g,a_2 \to a_4} & P_{g,a_3 \to a_4} & P_{g,a_4 \to a_4} \end{bmatrix} \times \begin{bmatrix} J_{in,g,1} \\ J_{in,g,2} \\ J_{in,g,3} \\ J_{in,g,4} \end{bmatrix} \tag{25}$$

A 4x4 response matrix $\mathbf{R}^I$ can thus be written for any subsystem I as:

$$\mathbf{R}^I = \begin{bmatrix} P^I_{g,a_1 \to a_1} & P^I_{g,a_2 \to a_1} & P^I_{g,a_3 \to a_1} & P^I_{g,a_4 \to a_1} \\ P^I_{g,a_1 \to a_2} & P^I_{g,a_2 \to a_2} & P^I_{g,a_3 \to a_2} & P^I_{g,a_4 \to a_2} \\ P^I_{g,a_1 \to a_3} & P^I_{g,a_2 \to a_3} & P^I_{g,a_3 \to a_3} & P^I_{g,a_4 \to a_3} \\ P^I_{g,a_1 \to a_4} & P^I_{g,a_2 \to a_4} & P^I_{g,a_3 \to a_4} & P^I_{g,a_4 \to a_4} \end{bmatrix} \tag{26}$$

Since the probability to go from a surface back to the same surface is zero, the diagonal of each $\mathbf{R}^I$ matrix will be 0 and we finally get:

$$\mathbf{R}^I = \begin{bmatrix} 0 & P^I_{g,a_2 \to a_1} & P^I_{g,a_3 \to a_1} & P^I_{g,a_4 \to a_1} \\ P^I_{g,a_1 \to a_2} & 0 & P^I_{g,a_3 \to a_2} & P^I_{g,a_4 \to a_2} \\ P^I_{g,a_1 \to a_3} & P^I_{g,a_2 \to a_3} & 0 & P^I_{g,a_4 \to a_3} \\ P^I_{g,a_1 \to a_4} & P^I_{g,a_2 \to a_4} & P^I_{g,a_3 \to a_4} & 0 \end{bmatrix} \tag{27}$$

The response matrix for the entire system made of N subsystems is then constructed as follows:

$$\mathbf{R} = \begin{bmatrix} \mathbf{R}^1 & 0 & 0 \\ 0 & \ddots & 0 \\ 0 & 0 & \mathbf{R}^N \end{bmatrix} \tag{28}$$

5.3.2 Building of the matrix $\mathbf{P}$

In order to relate the incoming neutron currents to the outgoing currents, a topological matrix $\mathbf{P}$ is used, as generically expressed by Eq. (10). This matrix is square with the same number of rows and columns as there are surface currents. Building the $\mathbf{P}$ matrix is heavily dependent on the labelling of the system since a different labelling procedure results in a different $\mathbf{P}$ matrix. The $\mathbf{P}$ matrix also considers the boundary condition applied (i.e. reflective boundary condition in the present case). Using the labelling of the system as earlier detailed and the illustrative example of a 2x2 system, the $\mathbf{P}$ matrix is given by, dropping the energy group labelling:

$$\begin{bmatrix} J_{in,1} \\ J_{in,2} \\ J_{in,3} \\ J_{in,4} \\ J_{in,5} \\ J_{in,6} \\ J_{in,7} \\ J_{in,8} \\ J_{in,9} \\ J_{in,10} \\ J_{in,11} \\ J_{in,12} \\ J_{in,13} \\ J_{in,14} \\ J_{in,15} \\ J_{in,16} \end{bmatrix} = \begin{bmatrix} 1 & 0 & 0 & 0 & 0 & 0 & 0 & 0 & 0 & 0 & 0 & 0 & 0 & 0 & 0 & 0 \\ 0 & 1 & 0 & 0 & 0 & 0 & 0 & 0 & 0 & 0 & 0 & 0 & 0 & 0 & 0 & 0 \\ 0 & 0 & 0 & 0 & 0 & 0 & 0 & 0 & 1 & 0 & 0 & 0 & 0 & 0 & 0 & 0 \\ 0 & 0 & 0 & 0 & 0 & 1 & 0 & 0 & 0 & 0 & 0 & 0 & 0 & 0 & 0 & 0 \\ 0 & 0 & 0 & 0 & 1 & 0 & 0 & 0 & 0 & 0 & 0 & 0 & 0 & 0 & 0 & 0 \\ 0 & 0 & 0 & 1 & 0 & 0 & 0 & 0 & 0 & 0 & 0 & 0 & 0 & 0 & 0 & 0 \\ 0 & 0 & 0 & 0 & 0 & 0 & 0 & 0 & 0 & 0 & 0 & 0 & 1 & 0 & 0 & 0 \\ 0 & 0 & 0 & 0 & 0 & 0 & 0 & 1 & 0 & 0 & 0 & 0 & 0 & 0 & 0 & 0 \\ 0 & 0 & 1 & 0 & 0 & 0 & 0 & 0 & 0 & 0 & 0 & 0 & 0 & 0 & 0 & 0 \\ 0 & 0 & 0 & 0 & 0 & 0 & 0 & 0 & 0 & 1 & 0 & 0 & 0 & 0 & 0 & 0 \\ 0 & 0 & 0 & 0 & 0 & 0 & 0 & 0 & 0 & 0 & 1 & 0 & 0 & 0 & 0 & 0 \\ 0 & 0 & 0 & 0 & 0 & 0 & 0 & 0 & 0 & 0 & 0 & 0 & 0 & 1 & 0 & 0 \\ 0 & 0 & 0 & 0 & 0 & 0 & 1 & 0 & 0 & 0 & 0 & 0 & 0 & 0 & 0 & 0 \\ 0 & 0 & 0 & 0 & 0 & 0 & 0 & 0 & 0 & 0 & 0 & 1 & 0 & 0 & 0 & 0 \\ 0 & 0 & 0 & 0 & 0 & 0 & 0 & 0 & 0 & 0 & 0 & 0 & 0 & 0 & 1 & 0 \\ 0 & 0 & 0 & 0 & 0 & 0 & 0 & 0 & 0 & 0 & 0 & 0 & 0 & 0 & 0 & 1 \end{bmatrix} \times \begin{bmatrix} J_{out,1} \\ J_{out,2} \\ J_{out,3} \\ J_{out,4} \\ J_{out,5} \\ J_{out,6} \\ J_{out,7} \\ J_{out,8} \\ J_{out,9} \\ J_{out,10} \\ J_{out,11} \\ J_{out,12} \\ J_{out,13} \\ J_{out,14} \\ J_{out,15} \\ J_{out,16} \end{bmatrix} \tag{29}$$

where at the boundaries of the system $J_{in} = 1 \times J_{out}$. For the other inner continuity conditions, one also has $J_{in} = 1 \times J_{out}$. As seen above, the $\mathbf{P}$ matrix is sparse and its determination is relatively simple once the labelling of the system has been chosen.

5.3.3 Building of the matrix $\mathbf{S}$

For the local problem generically expressed by Eq. (6), the structure of the $\mathbf{S}$ matrix, for the system considered in this work and made of two regions, can be determined from the following expression giving the neutron flux in region 1:

$$\phi_{1,g} = \frac{S_1 P_{g,a_1\to 1}}{\Sigma_{T,g,1} V_1} \cdot J_{in,g,1} + \frac{S_2 P_{g,a_2\to 1}}{\Sigma_{T,g,1} V_1} \cdot J_{in,g,2} + \frac{S_3 P_{g,a_3\to 1}}{\Sigma_{T,g,1} V_1} \cdot J_{in,g,3} + \frac{S_4 P_{g,a_4\to 1}}{\Sigma_{T,g,1} V_1} \cdot J_{in,g,4} \tag{30}$$

and from a similar expression for the neutron flux in region 2. One thus obtains:

$$\begin{bmatrix} \phi_{1,g} \\ \phi_{2,g} \end{bmatrix} = \begin{bmatrix} \frac{S_1 P_{g,a_1\to 1}}{\Sigma_{T,g,1} V_1} & \frac{S_2 P_{g,a_2\to 1}}{\Sigma_{T,g,1} V_1} & \frac{S_3 P_{g,a_3\to 1}}{\Sigma_{T,g,1} V_1} & \frac{S_4 P_{g,a_4\to 1}}{\Sigma_{T,g,1} V_1} \\ \frac{S_1 P_{g,a_1\to 2}}{\Sigma_{T,g,2} V_2} & \frac{S_2 P_{g,a_2\to 2}}{\Sigma_{T,g,2} V_2} & \frac{S_3 P_{g,a_3\to 2}}{\Sigma_{T,g,2} V_2} & \frac{S_4 P_{g,a_4\to 2}}{\Sigma_{T,g,2} V_2} \end{bmatrix} \times \begin{bmatrix} J_{in,g,1} \\ J_{in,g,2} \\ J_{in,g,3} \\ J_{in,g,4} \end{bmatrix} \tag{31}$$

with the $\mathbf{S}^I$ matrix for the subsystem I having for dimensions 2x4 and expressed as:

$$\mathbf{S}^I = \begin{bmatrix} \frac{S_1 P^I_{g,a_1\to 1}}{\Sigma_{T,g,1} V_1} & \frac{S_2 P^I_{g,a_2\to 1}}{\Sigma_{T,g,1} V_1} & \frac{S_3 P^I_{g,a_3\to 1}}{\Sigma_{T,g,1} V_1} & \frac{S_4 P^I_{g,a_4\to 1}}{\Sigma_{T,g,1} V_1} \\ \frac{S_1 P^I_{g,a_1\to 2}}{\Sigma_{T,g,2} V_2} & \frac{S_2 P^I_{g,a_2\to 2}}{\Sigma_{T,g,2} V_2} & \frac{S_3 P^I_{g,a_3\to 2}}{\Sigma_{T,g,2} V_2} & \frac{S_4 P^I_{g,a_4\to 2}}{\Sigma_{T,g,2} V_2} \end{bmatrix} \tag{32}$$

For the entire system, the $\mathbf{S}$ matrix then consists on the diagonal of blocks of $\mathbf{S}^I$ submatrices for each of the N subsystems and zeros otherwise:

$$\mathbf{S} = \begin{bmatrix} \mathbf{S}^1 & 0 & 0 \\ 0 & \ddots & 0 \\ 0 & 0 & \mathbf{S}^N \end{bmatrix} \tag{33}$$

5.3.4 Building of the matrix $\mathbf{F}$

The matrix $\mathbf{F}$ can be built from examining Eq. (14), which can, for illustration purposes, be explicitly written in the case of the fuel region being considered and in the energy group 1 as:

$$\begin{aligned} x_{1,fuel} &= V_{fuel} P_{1,fuel\to fuel} \chi_{1,fuel} (\nu\Sigma_{f,1,fuel}) \times \phi_{1,fuel} + V_{fuel} P_{1,fuel\to fuel} \chi_{1,fuel} (\nu\Sigma_{f,2,fuel}) \times \phi_{2,fuel} \\ &+ V_{mod} P_{1,mod\to fuel} \chi_{1,mod} (\nu\Sigma_{f,1,mod}) \times \phi_{1,mod} + V_{mod} P_{1,mod\to fuel} \chi_{1,mod} (\nu\Sigma_{f,2,mod}) \times \phi_{2,mod} \end{aligned} \tag{34}$$

Doing the same for any region and any energy group, and writing the expressions in a matrix form, the following equation is obtained:

$$\begin{bmatrix} x_{1,fuel} \\ x_{2,fuel} \\ x_{1,mod} \\ x_{2,mod} \end{bmatrix} =$$

$$\begin{bmatrix} V_{fuel}P_{1,fuel\to fuel}\chi_{1,fuel}(\nu\Sigma_{f,1,fuel}) & V_{fuel}P_{1,fuel\to fuel}\chi_{1,fuel}(\nu\Sigma_{f,2,fuel}) & V_{mod}P_{1,mod\to fuel}\chi_{1,mod}(\nu\Sigma_{f,1,mod}) & V_{mod}P_{1,mod\to fuel}\chi_{1,mod}(\nu\Sigma_{f,2,mod}) \\ V_{fuel}P_{2,fuel\to fuel}\chi_{2,fuel}(\nu\Sigma_{f,1,fuel}) & V_{fuel}P_{2,fuel\to fuel}\chi_{2,fuel}(\nu\Sigma_{f,2,fuel}) & V_{mod}P_{2,mod\to fuel}\chi_{2,mod}(\nu\Sigma_{f,1,mod}) & V_{mod}P_{2,mod\to fuel}\chi_{2,mod}(\nu\Sigma_{f,2,mod}) \\ V_{fuel}P_{1,fuel\to \mathrm{mod}}\chi_{1,fuel}(\nu\Sigma_{f,1,fuel}) & V_{fuel}P_{1,fuel\to \mathrm{mod}}\chi_{1,fuel}(\nu\Sigma_{f,2,fuel}) & V_{mod}P_{1,mod\to \mathrm{mod}}\chi_{1,mod}(\nu\Sigma_{f,1,mod}) & V_{mod}P_{1,mod\to \mathrm{mod}}\chi_{1,mod}(\nu\Sigma_{f,2,mod}) \\ V_{fuel}P_{2,fuel\to \mathrm{mod}}\chi_{2,fuel}(\nu\Sigma_{f,1,fuel}) & V_{fuel}P_{2,fuel\to \mathrm{mod}}\chi_{2,fuel}(\nu\Sigma_{f,2,fuel}) & V_{mod}P_{2,mod\to \mathrm{mod}}\chi_{2,mod}(\nu\Sigma_{f,1,mod}) & V_{mod}P_{2,mod\to \mathrm{mod}}\chi_{2,mod}(\nu\Sigma_{f,2,mod}) \end{bmatrix}$$

$$\times \begin{bmatrix} \phi_{1,fuel} \\ \phi_{2,fuel} \\ \phi_{1,mod} \\ \phi_{2,mod} \end{bmatrix} \tag{35}$$

The matrix $\mathbf{F}^I$ for the subsystem is thus given by:

$$\mathbf{F}^I =$$

$$\begin{bmatrix} V_{fuel}P^I_{1,fuel\to fuel}\chi_{1,fuel}(\nu\Sigma_{f,1,fuel}) & V_{fuel}P^I_{1,fuel\to fuel}\chi_{1,fuel}(\nu\Sigma_{f,2,fuel}) & V_{mod}P^I_{1,mod\to fuel}\chi_{1,mod}(\nu\Sigma_{f,1,mod}) & V_{mod}P^I_{1,mod\to fuel}\chi_{1,mod}(\nu\Sigma_{f,2,mod}) \\ V_{fuel}P^I_{2,fuel\to fuel}\chi_{2,fuel}(\nu\Sigma_{f,1,fuel}) & V_{fuel}P^I_{2,fuel\to fuel}\chi_{2,fuel}(\nu\Sigma_{f,2,fuel}) & V_{mod}P^I_{2,mod\to fuel}\chi_{2,mod}(\nu\Sigma_{f,1,mod}) & V_{mod}P^I_{2,mod\to fuel}\chi_{2,mod}(\nu\Sigma_{f,2,mod}) \\ V_{fuel}P^I_{1,fuel\to \mathrm{mod}}\chi_{1,fuel}(\nu\Sigma_{f,1,fuel}) & V_{fuel}P^I_{1,fuel\to \mathrm{mod}}\chi_{1,fuel}(\nu\Sigma_{f,2,fuel}) & V_{mod}P^I_{1,mod\to \mathrm{mod}}\chi_{1,mod}(\nu\Sigma_{f,1,mod}) & V_{mod}P^I_{1,mod\to \mathrm{mod}}\chi_{1,mod}(\nu\Sigma_{f,2,mod}) \\ V_{fuel}P^I_{2,fuel\to \mathrm{mod}}\chi_{2,fuel}(\nu\Sigma_{f,1,fuel}) & V_{fuel}P^I_{2,fuel\to \mathrm{mod}}\chi_{2,fuel}(\nu\Sigma_{f,2,fuel}) & V_{mod}P^I_{2,mod\to \mathrm{mod}}\chi_{2,mod}(\nu\Sigma_{f,1,mod}) & V_{mod}P^I_{2,mod\to \mathrm{mod}}\chi_{2,mod}(\nu\Sigma_{f,2,mod}) \end{bmatrix} \tag{36}$$

For the entire system, the $\mathbf{F}$ matrix then consists on the diagonal of blocks of $\mathbf{S}^I$ submatrices for each of the N subsystems and zeros otherwise:

$$\mathbf{F} = \begin{bmatrix} \mathbf{F}^1 & 0 & 0 \\ 0 & \ddots & 0 \\ 0 & 0 & \mathbf{F}^N \end{bmatrix} \tag{37}$$

It should be mentioned that half of elements of the $\mathbf{F}^I$ matrices for the system investigated in this work are zeros, since there is no fission occurring in the moderator region.

5.3.5 Estimation of the emission density Q

In each region, the emission density Q can be calculated according to Eq. (4). In a two-energy group format, the emission density for energy group g and region i can be formally expressed as:

$$Q_{g,i} = \frac{1}{4\pi}\left[\Sigma_{s0,1\to g,i}\phi_{1,i} + \frac{\chi_{1,i}\nu\Sigma_{f,1,i}}{k_{eff}}\phi_{1,i} + \Sigma_{s0,2\to g,i}\phi_{2,i} + \frac{\chi_{2,i}\nu\Sigma_{f,2,i}}{k_{eff}}\phi_{2,i}\right] \tag{38}$$

In the moderator region, Eq. (38) will simplify since there is no fission and hence the second and fourth term will disappear.

5.3.6 Estimation of the source terms ϕ_{source} and $\mathbf{J}_{source}$

In the global problem given by Eq. (11), the contribution from the source currents needs to be calculated. Looking at the explicit version of the equation representing the global problem and given by Eq. (7), the contribution from the emission densities to outgoing currents on each surface can be determined, in a two-region formulation, as:

$$\begin{bmatrix} J_{out,g,1} \\ J_{out,g,2} \\ J_{out,g,3} \\ J_{out,g,4} \end{bmatrix} = \begin{bmatrix} P_{g,1\to a_1} & P_{g,2\to a_1} \\ P_{g,1\to a_2} & P_{g,2\to a_2} \\ P_{g,1\to a_3} & P_{g,2\to a_3} \\ P_{g,1\to a_4} & P_{g,2\to a_4} \end{bmatrix} \times \begin{bmatrix} \frac{V_1}{S} & 0 \\ 0 & \frac{V_2}{S} \end{bmatrix} \times \begin{bmatrix} Q_{g,1} \\ Q_{g,2} \end{bmatrix} \tag{39}$$

Likewise, in the local problem given by Eq. (12), the contribution from the source fluxes needs to be determined. Looking at the explicit version of the equation representing the local problem and given by Eq. (6), the source flux contribution will be given, in a two-region formulation, by:

$$\begin{bmatrix} \phi_{g,1}^{source} \\ \phi_{g,2}^{source} \end{bmatrix} = \begin{bmatrix} \frac{P_{g,1\to 1}}{\Sigma_{T,g,1}^0} & \frac{V_2 P_{g,2\to 1}}{V_1 \Sigma_{T,g,1}^0} \\ \frac{V_1 P_{g,1\to 2}}{V_2 \Sigma_{T,g,2}^0} & \frac{P_{g,2\to 2}}{\Sigma_{T,g,2}^0} \end{bmatrix} \times \begin{bmatrix} Q_{g,1} \\ Q_{g,2} \end{bmatrix} \tag{40}$$

6. Results

In the proposed hybrid method, which relies on the response matrix formulation, two sets of results/data are calculated: the neutron flux in each region of the system together with the corresponding dominant eigenvalue (using the deterministic framework) and the collision probabilities (using the probabilistic framework).

6.1 Results from the probabilistic framework

Based on the methodology described in this work, the Serpent2 code is used to estimate various probabilities: region-to-region first collision probabilities, region-to-surface escape probabilities, surface-to-region first collision probabilities, and surface-to-surface escape probabilities. In the case investigated in this work, such probabilities are estimated in a two-energy group structure and for elementary cells made of 2 regions (fuel and moderator, respectively) and having 4 outer surfaces (see Fig. 2). In addition, since the modelled fuel assembly contains 6 different fuel pin types (each with its own enrichment), these sets of probabilities need to be determined for each of the 6 fuel pin types. The complete sets of probabilities estimated from Serpent2 are given in Table 1 for neutrons emitted from the fuel region, in Table 2 for neutrons emitted from the moderator region and in Table 3 for neutrons emitted from an outer surface. The fact that the sum of the probabilities in Table 2 does not add up to exactly unity might be due to (n,2n) reactions not properly accounted for in the present methodology.

Table 1 Sets of probabilities for neutrons emitted from the fuel region. The results for the fast energy group are given in the upper half of the table, whereas the results for the thermal energy group are given in the lower half of the table.

Pin	$P_{fuel\to fuel}$	$P_{fuel\to mod}$	$P_{fuel\to a_1}$	$P_{fuel\to a_2}$	$P_{fuel\to a_3}$	$P_{fuel\to a_4}$	Sum
1	0.2148	0.1380	0.1618	0.1618	0.1618	0.1618	1.0000
2	0.2140	0.1384	0.1619	0.1619	0.1619	0.1619	1.0000
3	0.2147	0.1379	0.1619	0.1619	0.1619	0.1619	1.0000
4	0.2140	0.1383	0.1619	0.1619	0.1619	0.1619	1.0000
5	0.2154	0.1381	0.1616	0.1616	0.1616	0.1616	1.0000
6	0.2137	0.1381	0.1620	0.1620	0.1620	0.1620	1.0000
1	0.2453	0.2874	0.1168	0.1168	0.1168	0.1168	1.0000
2	0.2523	0.2846	0.1158	0.1158	0.1158	0.1158	1.0000
3	0.2615	0.2785	0.1150	0.1150	0.1150	0.1150	1.0000
4	0.2710	0.2742	0.1137	0.1137	0.1137	0.1137	1.0000
5	0.2755	0.2709	0.1134	0.1134	0.1134	0.1134	1.0000
6	0.2801	0.2686	0.1128	0.1128	0.1128	0.1128	1.0000

Table 2 Sets of probabilities for neutrons emitted from the moderator region. The results for the fast energy group are given in the upper half of the table, whereas the results for the thermal energy group are given in the lower half of the table.

Pin	$P_{mod\to mod}$	$P_{mod\to fuel}$	$P_{mod\to a_1}$	$P_{mod\to a_2}$	$P_{mod\to a_3}$	$P_{mod\to a_4}$	Sum
1	0.2582	0.0779	0.1652	0.1652	0.1656	0.1652	0.9973
2	0.2668	0.0784	0.1654	0.1652	0.1654	0.1656	1.0067
3	0.2780	0.0785	0.1654	0.1657	0.1657	0.1657	1.0188
4	0.2853	0.0790	0.1655	0.1656	0.1658	0.1658	1.0269
5	0.2912	0.0792	0.1658	0.1656	0.1659	0.1657	1.0334
6	0.2951	0.0794	0.1658	0.1659	0.1661	0.1658	1.0381
1	0.4168	0.0801	0.1320	0.1317	0.1319	0.1318	1.0243
2	0.4170	0.0827	0.1318	0.1318	0.1320	0.1316	1.0268
3	0.4173	0.0862	0.1318	0.1318	0.1320	0.1317	1.0309
4	0.4182	0.0890	0.1319	0.1316	0.1314	0.1319	1.0340
5	0.4193	0.0918	0.1315	0.1314	0.1315	0.1315	1.0370
6	0.4193	0.0939	0.1316	0.1314	0.1315	0.1317	1.0393

Table 3 Sets of probabilities for neutrons emitted from a surface. The results for the fast energy group are given in the upper half of the table, whereas the results for the thermal energy group are given in the lower half of the table.

Pin	$P_{a_1 \to a_1}$	$P_{a_1 \to a_2}$	$P_{a_1 \to a_3}$	$P_{a_1 \to a_4}$	$P_{a_1 \to fuel}$	$P_{a_1 \to mod}$	Sum
1	0	0.2170	0.2101	0.2097	0.1247	0.2385	1.0000
2	0	0.2172	0.2100	0.2100	0.1250	0.2378	1.0000
3	0	0.2173	0.2101	0.2101	0.1252	0.2373	1.0000
4	0	0.2174	0.2102	0.2104	0.1254	0.2366	1.0000
5	0	0.2176	0.2103	0.2105	0.1254	0.2362	1.0000
6	0	0.2173	0.2105	0.2104	0.1258	0.2360	1.0000
1	0	0.1078	0.1334	0.1336	0.1221	0.5031	1.0000
2	0	0.1081	0.1344	0.1338	0.1251	0.4987	1.0000
3	0	0.1061	0.1349	0.1344	0.1309	0.4938	1.0000
4	0	0.1048	0.1347	0.1352	0.1345	0.4908	1.0000
5	0	0.1037	0.1346	0.1347	0.1390	0.4880	1.0000
6	0	0.1034	0.1349	0.1346	0.1418	0.4853	1.0000

For the sake of completeness, the energy- and volume-averaged macroscopic cross-sections determined by Serpent 2 are also given in Table 4 for the fuel region and in Table 5 for the moderator region.

Table 4 Macroscopic cross-section data for the fuel region. The data for the fast energy group are given in the upper half of the table, whereas the data for the thermal energy group are given in the lower half of the table.

Pin	Σ_f $[\mathrm{cm}^{-1}]$	Σ_{tot} $[\mathrm{cm}^{-1}]$
1	0.0156	0.4229
2	0.0170	0.4236
3	0.0191	0.4243
4	0.0208	0.4249
5	0.0224	0.4257
6	0.0236	0.4260
1	0.2853	0.5732
2	0.3264	0.5926
3	0.3931	0.6243
4	0.4447	0.6489
5	0.4940	0.6724
6	0.5301	0.6897

Table 5 Macroscopic cross-section data for the moderator region. The data for the fast energy group are given in the upper half of the table, whereas the data for the thermal energy group are given in the lower half of the table.

Pin	Σ_{tot} $[\mathrm{cm}^{-1}]$
1	0.4065
2	0.4058
3	0.4045
4	0.4036
5	0.4029
6	0.4020
1	1.1163
2	1.1072
3	1.0941
4	1.0851
5	1.0766
6	1.0709

6.2 Results from the deterministic framework

With the probabilities and macroscopic data determined from Serpent2, the neutron currents, neutron fluxes, and the corresponding dominant eigenvalue can be determined using the response matrix method implemented in Matlab. Fig. 8 gives the spatial distribution of the converged scalar neutron fluxes for the fast and thermal energy groups, respectively, along a diagonal across the fuel assembly modelled in 2 dimensions.

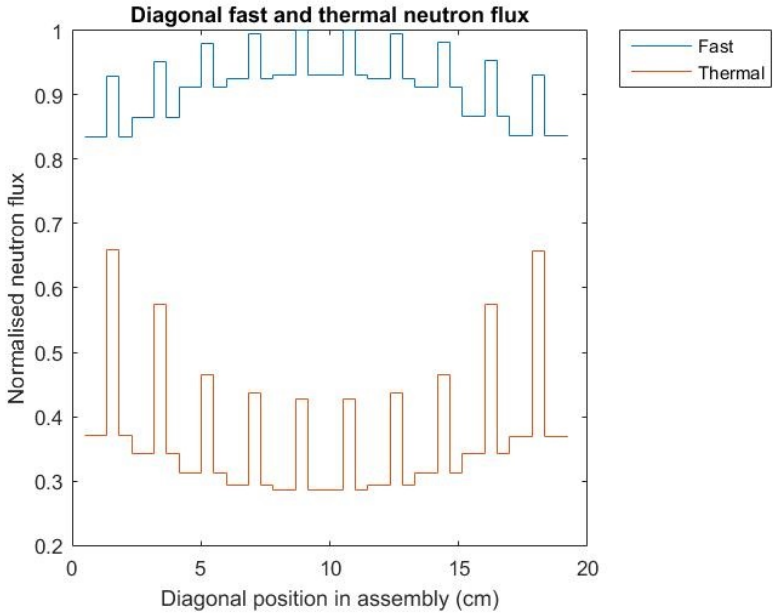

Fig. 8 Spatial distribution of the scalar neutron flux along a diagonal across the modelled fuel assembly.

The symmetrical spatial distribution of the scalar neutron flux is explained by the symmetrical fuel assembly pattern used in the present demonstration, as can be seen in Fig. 1. It is worth mentioning that no assumption of symmetry was made in the deterministic framework. The computed scalar neutron is though symmetrical, as it should be because of the symmetrical nature of the arrangement of the fuel pins. It is also observed that the neutron fluxes are highest in the fuel regions (peaks) and lowest in the moderator regions (dips), for both the fast and thermal energy groups. A finer spatial mesh in the moderator and fuel regions would result in a more faithful representation of the neutron flux gradients.

It can also be noticed that the fast neutron flux is highest in the middle of the fuel assembly and the thermal neutron flux is lowest at that location. This is explained by the fact that the central part of the fuel assembly contains the fuel pins having the highest enrichment. This will lead to a neutron flux depression at that location at thermal energies (due to increased thermal absorptions) and to an increased neutron flux level at fast energies (due to higher release of fission neutrons).

Finally, one notices that the neutron flux flattens out towards the edges of the system. This is the result of the reflective boundary condition used: the net neutron currents across the boundary is zero, resulting in a flat flux distribution.

In terms of multiplication factor, the solver converges to $k_{\infty} = 13.8$. Although the system modelled in Serpent2 differs from the one modelled in the present hybrid framework (coarse spatial mesh used and assumption of isotropic emissions in the hybrid framework), the Serpent2 multiplication factor is found to be $k_{\infty} = 1.15$. The dominant eigenvalue estimated by the hybrid solver significantly differs from Serpent2 and is unphysical. The reason for this discrepancy has not yet been found at the time of the writing of this report.

It is also interesting to look at the convergence in neutron flux and in the dominant eigenvalue. Fig. 9 gives the evolution of the relative difference between two successive iterations in neutron flux and in eigenvalue. The deterministic solver converges in 658 iterations for convergence criteria on neutron flux and eigenvalue both set to 10^{-6}.

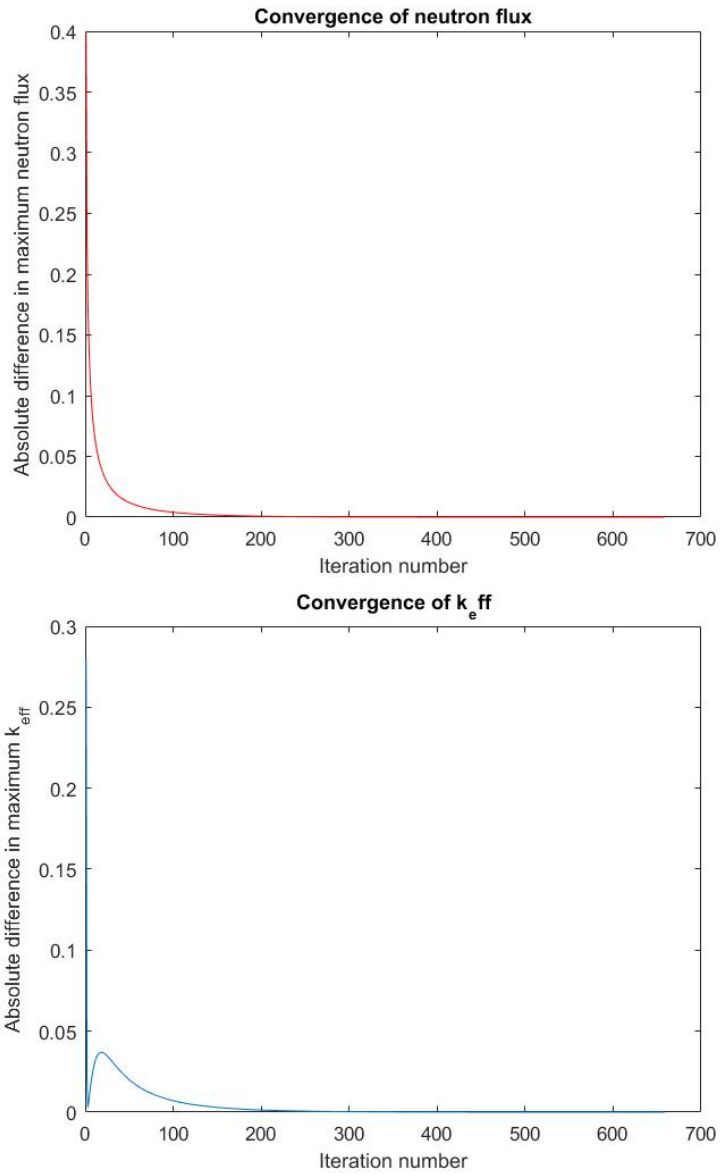

Fig. 9 Evolution of the absolute value of the relative difference in neutron flux (top figure) and in eigenvalue (bottom figure) as functions of the iteration number.

7. Conclusions and outlook

In this work, a new hybrid neutron transport method was proposed, developed and implemented. The framework makes use of a deterministic approach relying on the response matrix method for which the required probabilities are estimated from a probabilistic approach. For the probabilistic calculations, the Serpent2 Monte Carlo code was used and modified when necessary in order to make the calculations of the necessary probabilities possible. For the deterministic calculations, a response matrix formulation combined with a power iteration technique was implemented in Matlab.

The feasibility of such a hybrid route was successfully demonstrated in this project.

Nevertheless, it was demonstrated that the implementation carried out for a simplified two-dimensional model of a BWR fuel assembly did not lead to physically-sound results for the infinite multiplication factor of the system. The reason of this unexpected behaviour has not yet been found at the time of the writing of this report.

In addition to possible errors in coding, several other factors could contribute to a multiplication factor deviating from a reasonable value. First, the response matrix formulation assumes isotropic and homogeneous volumetric emissions and surface emissions. For light water reactors, scattering is known to be strongly anisotropic. Even if a transport correction of the macroscopic cross-sections is used, the assumption of isotropy might be questionable when the meshing of each cell is coarse (i.e. one fuel region only and one moderator region only). With the present meshing, the emission densities are thus assumed to be spatially homogeneous and isotropic on the entire fuel and moderator, respectively, regions. Likewise, neutrons entering through surfaces are assumed to have a homogeneous and isotropic distribution on each of the surfaces. A finer meshing of each region and each region might lead to an improved modelling of the spatial heterogeneities of the volumetric and surface emissions. Concerning the assumption of isotropy, the development of a response matrix formulation for higher orders of the angular neutron flux than its first moments (scalar neutron flux and neutron currents) might be necessary. Finally, a better understanding of the handling of source neutrons for scattering within a region in Serpent2 is required to ensure that the estimation of the corresponding probabilities, as described in this report, was properly carried out.

In the continuation of this project, further tests of the framework in its present form will be undertaken to understand the root cause of the unexpected behaviour in the computed dominant eigenvalue. Thereafter, a benchmark between the developed method and a reference solution obtained entirely from Monte Carlo on a two-dimensional test case will be performed. If successful, extension of the method to three dimensions will be investigated and, as for the two-dimensional case, a benchmark between the developed method and a reference solution obtained entirely from Monte Carlo will be set up.

8. References

Boyd, W R, Smith, K & Forget B. 2013. A massively parallel Method of Characteristic neutral particle transport code for GPUs. In: Proceedings of International Conference on Mathematics and Computational Methods Applied to Nuclear Science and Engineering (M&C2013), Sun Valley, ID, USA, May 5 – 9, 2013, on CD-ROM, American Nuclear Society, LaGrange Park, IL, USA.

Carbol, S. 2017. Development of a hybrid neutron transport method in 2 energy groups. MSc thesis report CTH-NT-326, Chalmers University of Technology, Gothenburg, Sweden.

Davidson, G C, Evans, T M., Jarrell, J J, Hamilton S P & Pandya T M. 2014. Massively parallel, three-dimensional transport solutions for the k-eigenvalue problem. Nuclear Science and Engineering. 177 (2): 112–125.

Demazière, C. 2013. International Journal of Nuclear Energy Science and Technology. Multi-physics modelling of nuclear reactors: current practices in a nutshell. 7 (4): 288–318.

Dufek, J & Anglart, H. 2014. Derivation of a stable coupling scheme for Monte Carlo burnup calculations with the thermal–hydraulic feedback. Annals of Nuclear Energy. 62: 260–263.

Dufek, J & Hoogenboom, J E. 2014. Description of a stable scheme for steady-state coupled Monte Carlo - thermal-hydraulic calculations. Annals of Nuclear Energy. 68: 1–3.

Ishii, K, Hino, T, Mitsuyasu, T & Aoyama, M. 2009. Three-dimensional direct response matrix method using a Monte Carlo calculation. Journal of Nuclear Science and Technology. 46 (3): 259 – 267.

Ivanov, A, Sanchez, V, Stieglitz R & Ivanov K. 2014. Internal multi-scale multi-physics coupled system for high fidelity simulation of light water reactors. Annals of Nuclear Energy. 66: 104 – 112.

Lee, M J, Joo, H G, Lee, D & Smith, K. 2014. Coarse mesh finite difference formulation for accelerated Monte Carlo eigenvalue calculation. Annals of Nuclear Energy. 65: 101–113.

Leppänen, J, Pusa, M, Viitanen, T, Valtavirta, V & Kaltiaisenaho, T. 2015. The Serpent Monte Carlo code: Status, development and applications in 2013. Annals of Nuclear Energy. 82: 142 – 150.

Li, L, Smith, K & Forget, B. 2014. A low order nonlinear transport acceleration scheme for the method of characteristics. In: Proceedings of PHYSOR 2014 - The Role of Reactor Physics toward a Sustainable Future, Kyoto, Japan, September 28 – October 3, 2014.

Lux, I & Koblinger, L. 1991. Monte Carlo particle transport methods: neutron and photons calculations. CRC Press, Boca Raton, FL, USA.

Moriwaki, M, Ishii, K, Maruyama, H & Aoyama, M. 1999. A new direct calculation method of response matrices using a Monte Carlo calculation. Journal of Nuclear Science and Technology. 36 (10): 877–887.

Roberts, D R, Ouisloumen, M, Kucukboyaci, V N & Ivanov, K N. 2010. Development of iterative transport – diffusion methodology for LWR analysis. In: Proceedings of International Conference on the Advances in Reactor Physics to Power the Nuclear Renaissance (PHYSOR 2010), Pittsburgh, PA, USA, May 9 – 14, 2010, on CD-ROM, American Nuclear Society, LaGrange Park, IL, USA.

Stacey, W M. 2001. Nuclear reactor physics. John Wiley & Sons, New York, NY, USA.

Stamm'ler, R J J & Abbate, M J. 1983. Methods of steady-state reactor physics in nuclear design. Academic Press, London, United Kingdom.

U.S. Department of Energy. 2015. https://cesar.mcs.anl.gov, accessed on March 10, 2015.

U.S. Department of Energy. 2015. http://www.casl.gov, accessed on March 10, 2015.

Wolters, E R, Larsen, E W & Martin, W R. 2011. Generalized hybrid Monte Carlo-CMFD methods for fission source convergence. In: Proceedings of International Conference on

Mathematics and Computational Methods Applied to Nuclear Science and Engineering (M&C2011), Rio de Janeiro, RJ, Brazil, May 8 – 12, 2011, Latin American Section/ American Nuclear Society.

Zhang, D & Rahnema, F. 2012. An efficient hybrid stochastic/deterministic coarse mesh neutron transport method. Annals of Nuclear Energy. 41: 1–11.

Bibliographic Data Sheet **NKS-387**

Title	Development of a hybrid neutron transport solver in 2 energy groups
Author(s)	Sebastian Carbol, Mikael Andersson, Christophe Demazière and Jaakko Leppänen
Affiliation(s)	Chalmers University of Technology and Technical Research Centre of Finland (VTT)
ISBN	978-87-7893-473-4
Date	April 2017
Project	NKS- R / HYBRID
No. of pages	27
No. of tables	5
No. of illustrations	9
No. of references	19
Abstract max. 2000 characters	This project investigates the feasibility of performing reactor physics calculations for nuclear cores using a hybrid neutron transport methodology, by combining deterministic and probabilistic modelling techniques. In the presented implementation, a deterministic response matrix method was developed in Matlab. The necessary probabilities appearing in the response matrix method were estimated in advance using a probabilistic solver – the Monte Carlo code Serpent2. Ultimately, the hybrid framework will combine the advantages of the deterministic approach (fast running calculations) with the ones of the probabilistic approach (high flexibility in modelling any geometry and high accuracy). In the response matrix method, two grids are used: one fine grid for estimating the scalar neutron flux and a coarse grid for computing the neutron currents on this grid. Because of the large efforts developing a new computational framework represents and because such a developmental work is error-prone, this first phase of the project implemented and tested the hybrid framework on a system as simple as possible: a two-dimensional representation of a simplified BWR fuel assembly. Such a choice was governed by the necessity to lower the computational time and to have a tractable system during the developmental phase of the framework. The development of the hybrid route was demonstrated to be feasible, after some modifications of the Serpent2 code. Although promising, the solution computed by the framework was demonstrated to be not fully realistic. Additional investigations are necessary to identify the root cause of the observed deviations from the expected physical behaviour of the system.
Key words	nuclear reactor calculations, neutron transport, deterministic methods, probabilistic methods, hybrid methods

Available on request from the NKS Secretariat, P.O.Box 49, DK-4000 Roskilde, Denmark.
Phone (+45) 4677 4041, e-mail nks@nks.org, www.nks.org